Zhu *et al. Phytopathology Research* (2022) 4:16
https://doi.org/10.1186/s42483-022-00121-5

Phytopathology Research

RESEARCH Open Access

Deciphering the genome of *Simplicillium aogashimaense* to understand its mechanisms against the wheat powdery mildew fungus *Blumeria graminis* f. sp. *tritici*

Mo Zhu[1,2*], Xiao Duan[1], Pengkun Cai[1], Yong-fang Li[1,2] and Zongbo Qiu[1,2*]

Abstract

Simplicillium spp. are mycoparasites that exert growth-inhibitory effects on phytopathogenic fungi. However, limited studies have examined the effects of *Simplicillium* spp. on powdery mildews. In this study, morphological and molecular analyses revealed that *S. aogashimaense* is a mycoparasite of the wheat powdery mildew fungus, *Blumeria graminis* f. sp. *tritici* (*Bgt*), under field conditions. The inoculation of *Bgt* colonies with *S. aogashimaense* significantly impaired *Bgt* colony formation and conidial distribution and markedly decreased the biomass of *Bgt*. To examine the interaction between *Simplicillium* and *Bgt*, an *S. aogashimaense* strain that constitutively expresses green fluorescent protein (GFP) was constructed using the *Agrobacterium tumefaciens*-mediated transformation (ATMT) method. The hyphae of GFP-expressing *S. aogashimaense* directly penetrated the *B. graminis* structures. These findings indicate that ATMT can be employed to reveal the biocontrol activities of physiologically and phylogenetically diverse *Simplicillium* spp. In vitro, *S. aogashimaense* exudates compromised *Bgt* conidial germination and appressorial formation. Thus, *S. aogashimaense* functions as a potential biological control agent by impeding the development of *Bgt* and can be a viable alternative for controlling the wheat powdery mildew. To gain further insights into the mechanism underlying this mycoparasitism, the genome of *S. aogashimaense* was sequenced and assembled. *S. aogashimaense* harbored seven chromosomes comprising 8963 protein-coding genes. Additionally, two putative effector-coding genes (*Sao008714* and *Sao006491*) were identified. The expression levels of *Sao008714* and *Sao006491* in *S. aogashimaense* were dramatically upregulated during the mycoparasitic interaction. In addition, 41 gene clusters putatively involved in the production of secondary metabolites, which exhibit insecticidal, antifungal and antibacterial activities, were identified using genome-wide identification, annotation and analysis of secondary metabolite biosynthesis gene clusters. These results suggest that *S. aogashimaense* parasitizes *Bgt* and hence, can be considered for phytopathogen management.

Keywords: Wheat powdery mildew, Biological control, *Simplicillium aogashimaense*, ITS, Fungal identification

Background

Blumeria graminis f. sp. *tritici* (*Bgt*), an obligate biotrophic ascomycete, infests wheat and causes a destructive foliar disease. *Bgt*, which is associated with severe economic losses, is the sixth most crucial fungal phytopathogen worldwide (Dean et al. 2012). Currently, *B. graminis* is most effectively managed by the use of

*Correspondence: zhumo@htu.edu.cn; qiuzongbo@126.com
[1] College of Life Sciences, Henan Normal University, 46# East of Construction Road, Xinxiang 453007, Henan, People's Republic of China
Full list of author information is available at the end of the article

various chemical fungicides, however, this may pose risks to human health and the environment. Moreover, *B. graminis* has a high risk to develop resistance to several fungicides (FRAC Pathogen Risk List, www.frac.info, 2019). Therefore, some studies have focused on developing sustainable biological alternatives for controlling *B. graminis* (Kiss 2003; Köhl et al. 2019; Zhu et al. 2019). Recently, the potential of antagonists for biological control of powdery mildew diseases in several crops and ornamental plants has been explored owing to their environmentally friendly characteristics (Neveu et al. 2007; Belanger et al. 2012; Matzen et al. 2019; Németh et al. 2019). However, previous studies on biocontrol agents (BCAs) for powdery mildew diseases have mainly focused on the following species: *Verticillium lecanii*, *Pseudozyma flocculosa*, *Amphelomyces quisqualis* and *Tilletiopsis* spp. (Dik et al. 1998), and no known biological control products have been developed for cereal powdery mildew disease (Köhl et al. 2019). Thus, there is a need to identify novel BCAs.

Conidia and ascospores are important propagules in the pathogenesis of powdery mildew fungi. *B. graminis* mainly undergoes asexual propagation during disease development through repeatedly producing conidia (Zhu et al. 2017). Upon reaching a suitable host leaf surface, the conidia and ascospores of *B. graminis* germinate and then form the appressorium, an infection structure, to penetrate its hosts. After successful infection and haustorium formation, both conidial and ascosporic colonies produce young conidiophores with conidia that can serve as inocula for infection of volunteer plants (Jankovics et al. 2015). Therefore, conidial production and distribution play crucial roles in the pathogenesis of *B. graminis.*

Simplicillium species are ecologically and economically valuable due to their broad range of hosts and substrates (such as plants, insects, nematodes, human tissues and fungi), varied lifecycle, bioactive compound production and biocontrol activities (Wei et al. 2019). So far, at least 15 *Simplicillium* species have been identified. Some *Simplicillium* species are reported to be valuable BCAs for fungal phytopathogens. *S. lanosoniveum* exhibits mycophilic and disease-suppressive properties on rust fungus (*Phakopsora pachyrhizi*)-infected soybean leaves (Ward et al. 2012; Gauthier et al. 2014). Similar findings were documented by studies examining the growth-inhibitory effects of *S. aogashimaense* against *Puccinia* rust pathogens (i.e. *P. triticina*, *P. hordei* and *P. coronata* f. sp. *avenae*), *Bipolaris sorokiniana*, *Alternaria alternata* and *Curvularia trifolii* (Teasdale et al. 2018; Wilson et al. 2020). *S. lamellicola* has been demonstrated to decrease the incidence of gray mold disease (*Botrytis cinerea*) in tomato and ginseng (Shin et al. 2017). Meanwhile, *S. obclavatum*, a hyperparasite, affects the infection dynamics of the wheat strip rust fungus, *Puccinia striiformis* f. sp. *tritici* (Wang et al. 2020). Additionally, exudates of *S. lanosoniveum* exert antifungal potencies against pathogens causing brassica dark leaf spot (*Alternaria brassicicola*), rice brown spot (*Cochliobolus miyabeanus*) and the jasmine orange powdery mildew fungus (*Oidium murrayae*) in vitro (Chen et al. 2017). Cyclic peptides isolated from *S. obclavatum* exhibit potent growth-inhibitory activities against *Curvularia australiensis* (Liang et al. 2017). Thus, *Simplicillium* species are potential BCAs as they are capable of efficiently parasitizing and/or suppressing phytopathogens. However, the ability of *Simplicillium* species to parasitize powdery mildew fungi, including *B. graminis*, has not been previously reported.

Next generation sequencing has revolutionized the research on antagonistic microorganisms and phytopathogenic fungi. Previously, the genomes of some biological agents (i.e. *P. flocculosa* and *A. quisqualis*) were sequenced and the molecular mechanisms of antagonistic activities were illustrated (Lefebvre et al. 2013; Siozios et al. 2015; Laur et al. 2018). Although *Simplicillium* species are repeatedly shown antifungal activities against fungal pathogens, the underlying antifungal mechanisms have not been elucidated owing to the limited information on their genomes (Jauregui et al. 2020).

Identification of mycoparasites that are capable of parasitizing cereal pathogenic fungi is critical for developing BCAs against these pathogens. This study characterized a *Simplicillium* species isolated from *Bgt*-infected wheat leaves in a natural environment, which was identified as *S. aogashimaense* via morphological and molecular analyses. Since limited information is available on the mycophilic and disease-suppressive properties of *S. aogashimaense* in *Bgt* infection, and no studies have examined the interaction between fluorescence protein-transformed *Simplicillium* species and powdery mildew fungi, the characteristics and environmental fate of *Simplicillium* fungi before and after parasitizing powdery mildew pathogens are therefore still underestimated. Thus, in this study, we aimed to determine whether *S. aogashimaense* can efficiently parasitize *Bgt* colonies and to analyze the suppressive effects of *S. aogashimaense* on *Bgt* sporulation by quantifying the biomass during fungal-fungal interactions. Furthermore, the complete chromosome-scale genome of *S. aogashimaense* was elucidated, which is the first assembled genome of *Simplicillium* spp. A green fluorescent protein (GFP)-transformed strain of *S. aogashimaense* was constructed using the *Agrobacterium tumefaciens*-mediated transformation (ATMT) system to gain novel insights into the interactions between this BAC and *Bgt*.

Results

Identification of *S. aogashimaense* as a mycoparasite in *Bgt* colony

The morphological characteristics of *Bgt* colonies on wheat leaves were examined. Compared with *Bgt* colonies in their natural states on wheat leaves (Fig. 1a–d), aberrant colonies that turned from white to brownish color were observed (Fig. 1e), and the powdery mass significantly decreased in the aberrant colonies (Fig. 1f). To examine if these changes were caused by parasitization, *Bgt*-infected wheat leaves were examined. Microscopic analysis revealed that *Bgt* colonies were collapsed and covered by colonies of another fungus (Fig. 1g). Additionally, conidial production of *Bgt* was suppressed. Furthermore, *Bgt* conidia were surrounded and trapped by the hyphae of this fungus. Scanning electron microscopy analysis revealed similar findings. The fungus formed colonies, hyphae and conidia on *Bgt* colonies. The conidiophores of *Bgt* were collapsed, which impaired sporulation. *Bgt* conidia were also surrounded by hyphae of the fungus (Fig. 1h). Therefore, this fungus was identified as a mycoparasite of *Bgt*.

To identify the hyperparasite on *Bgt*-infected wheat leaves, the morphological characteristics of the purified mycoparasite were examined. The mycoparasite colonies on potato dextrose agar (PDA) exhibited a floccose-white color, while the reverse side exhibited a yellowish-white color (Fig. 2a, b). Conidia in small globose heads were formed at the apex of phialides on the aerial hyphae (Fig. 2c). The length and width of cylindrical conidia were 4.2–6.6 μm and 1.2–2.1 μm, respectively (Fig. 2d–f). Based on these morphological characteristics, this parasitic fungus was initially identified as *S. aogashimaense*. The internal transcribed spacer (ITS) region of this fungus was then sequenced. The sequence (GenBank accession no. MT936440) exhibited 99.49% identity with that of the previously reported *S. aogashimaense.* Phylogenetic analysis revealed that *S. aogashimaense* (AB604002) and the identified fungus clustered in the same branch (Fig. 2g). Therefore, the isolated fungus was confirmed to be *S. aogashimaense* based on morphological and molecular analyses.

Mycoparasitism of *S. aogashimaense* on *Bgt*

To confirm the ability of *S. aogashimaense* to parasitize *Bgt*, a mycoparasitism assay was performed. *Bgt*-infected and healthy wheat leaves were inoculated with *S. aogashimaense* spore suspension (1×10^6 spores/mL) or water and incubated in a growth chamber. The water-treated *Bgt* colonies did not exhibit morphological changes at all three time points tested (Fig. 3a–c). However, when inoculated with *S. aogashimaense*, this parasite formed hyphae and produced spores at 3 days post-inoculation (dpi) on *Bgt*-infected leaves (Fig. 3d); *Bgt* colonies were covered with *S. aogashimaense* at 6 dpi (Fig. 3e); crumbled conidiophores of *Bgt* were observed upon *S. aogashimaense* inoculation, and the number of *Bgt* conidia markedly decreased at 9 dpi (Fig. 3f). In comparison, no *S. aogashimaense* structures were observed on healthy leaf surfaces at these time points.

Next, the spores of GFP-transformed and wild-type (untransformed) *S. aogashimaense* were separately inoculated onto *Bgt*-infected wheat leaves and examined under a fluorescence microscope (Fig. 4). The

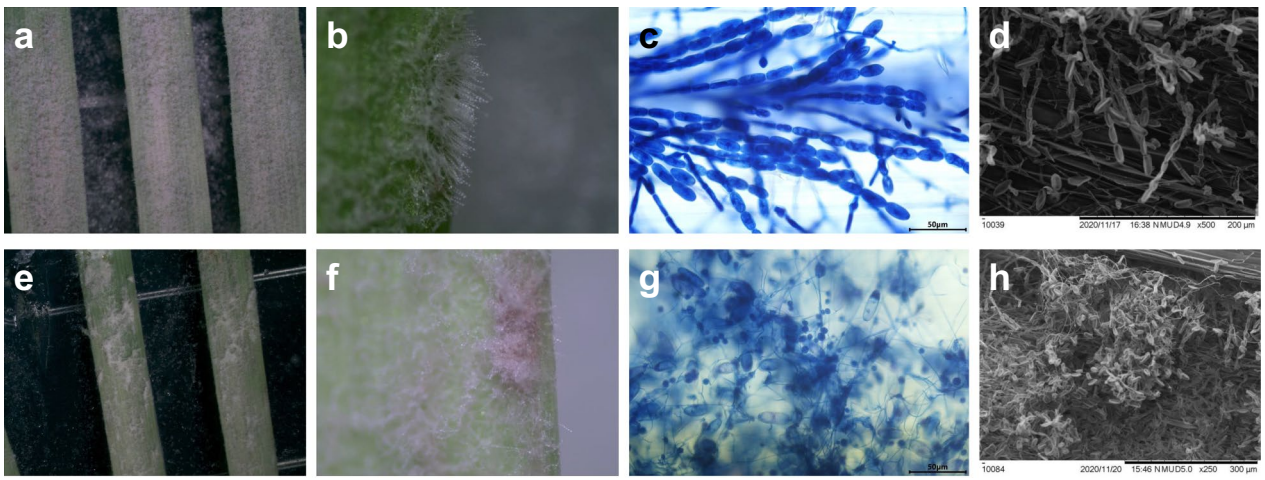

Fig. 1 Morphological characteristics of *Blumeria graminis* f. sp. *tritici* (*Bgt*) colonies. **a**–**d** Natural *Bgt* colonies. **e**–**h** Parasitized *Bgt* colonies. The colonies were monitored under a stereomicroscope (**a**, **b**, **e**, **f**), light microscope (**c**, **g**) and scanning electron microscope (**d**, **h**). Scale bars = 50 (**c**, **g**), 200 (**d**), or 300 μm (**h**)

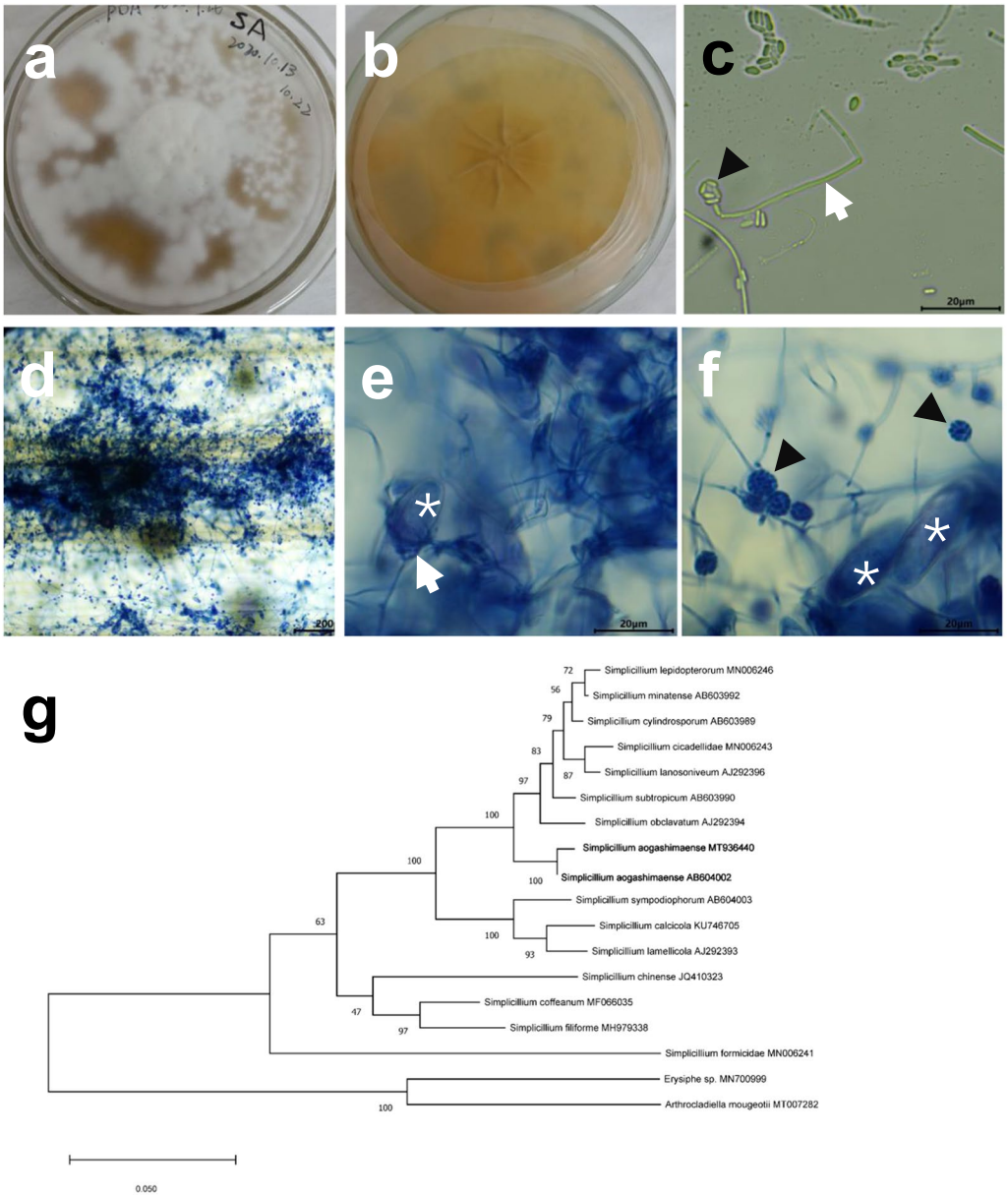

Fig. 2 Morphological characteristics and phylogenetical analysis of *Simplicillium aogashimaense*. **a**, **b** *S. aogashimaense* colonies on potato dextrose agar (PDA) at 9 dpi. **c** Mycelia and conidia of *S. aogashimaense*. **d**–**f** The interaction between *S. aogashimaense* and *Blumeria graminis* f. sp. *tritici* (*Bgt*) on wheat leaves. White and black arrows indicate mycelia and conidia (in globose head) of *S. aogashimaense*, respectively. White asterisks indicate conidia of *Bgt*. Scale bars = 20 (**c**, **e**, **f**) and 200 μm (**d**). **g** The phylogeny tree of the identified *S. aogashimaense* (MT936440) in this study and related *Simplicillium* species. The tree was constructed using the maximum likelihood method with MEGA software, with the options of 1000 bootstrap replicates, Tamura-Nei model and 50% site coverage cut-off. The *S. aogashimaense* (MT936440 and AB604002) strains are highlighted in bold. The bar indicates a distance of 0.050

results revealed that *S. aogashimaense* infected *Bgt*. Additionally, the mycoparasitism of wild-type and GFP-transformed strains was not markedly different.

Exudates of *S. aogashimaense* suppress *Bgt* growth

To determine if *S. aogashimaense* released growth-inhibitory metabolites against *Bgt*, the exudates of *S.*

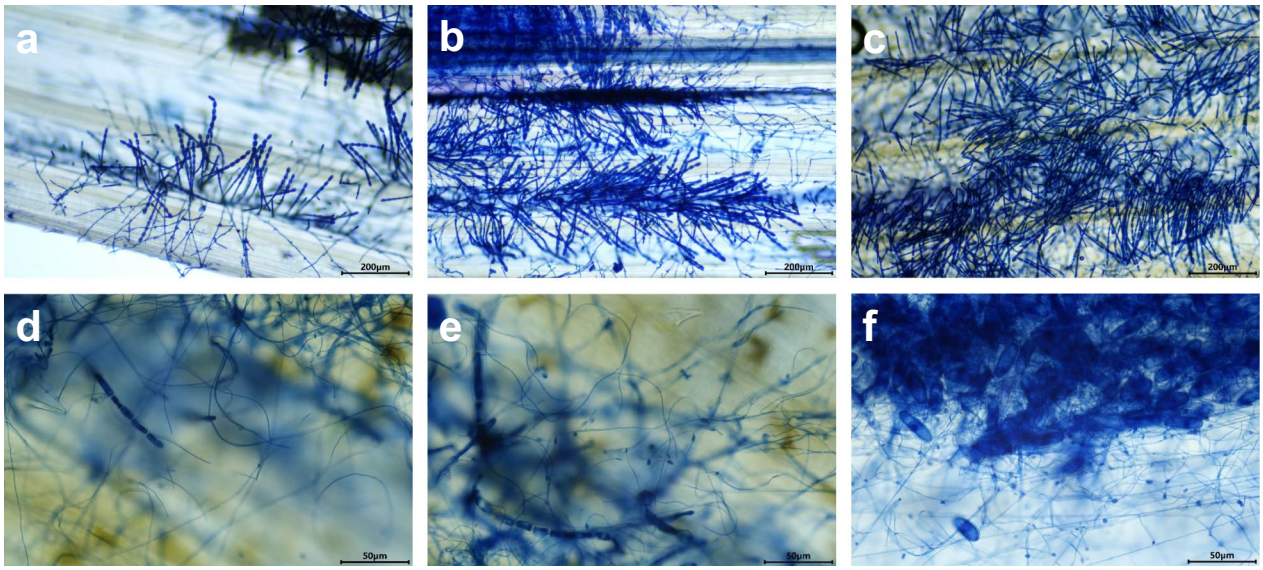

Fig. 3 Colonies of *Blumeria graminis* f. sp. *tritici* (*Bgt*). **a**–**c** *Bgt* colonies treated with water at 3, 6 and 9 dpi. **d**–**f** *Bgt* colonies treated with *S. aogashimaense* spore suspension at 3, 6 and 9 dpi, respectively. Scale bar = 200 (**a**–**c**) and 50 μm (**d**–**f**)

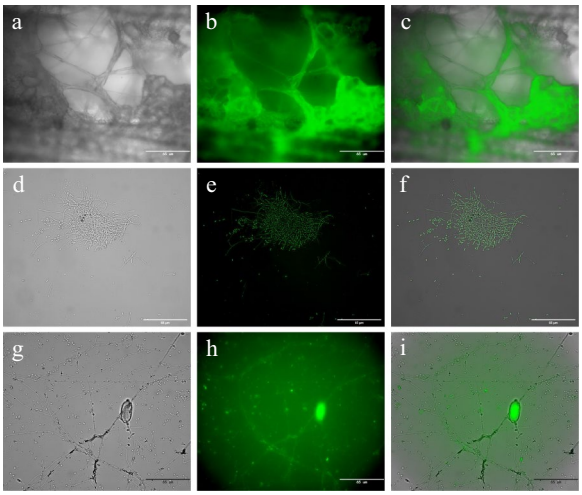

Fig. 4 Visualization of interaction between green fluorescent protein (GFP)-transformed *Simplicillium aogashimaense* and *Blumeria graminis* f. sp. *tritici* (*Bgt*). **a**–**c** Mycelia of transformed *S. aogashimaense* on *Bgt*-infected wheat leaves. **d**–**f** Mycelia and conidia of transformed *S. aogashimaense*. **g**–**i** The interaction between GFP transformed *S. aogashimaense* and a *Bgt* conidium. **a**, **d**, **g**, bright field images; **b**, **e**, **h**, fluorescence images; **c**, **f**, **i**, merged images. Scale bar = 65 μm

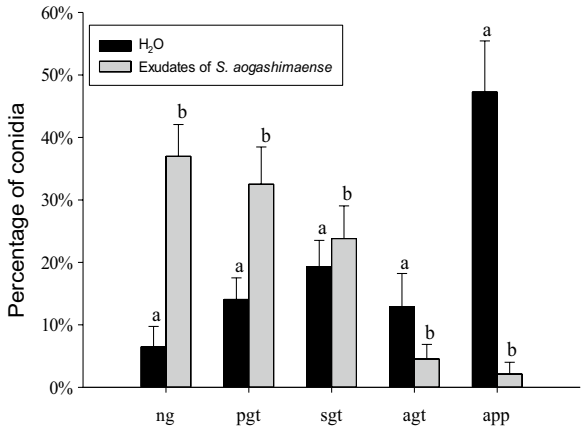

Fig. 5 Suppression effects of *Simplicillium aogashimaense* exudates on developmental processes of *Blumeria graminis* f. sp. *tritici* (*Bgt*) conidia in vitro. ng, non-germinated conidium; pgt, germinated conidium with only a primary germ tube; sgt, germinated conidium with an elongated secondary germ tube; agt, conidium with a swollen appressorial germ tube; app, conidium with a fully differentiated appressorium. Data are represented as mean ± standard deviation from five replicates (100 conidia each) of three independent biological experiments. The means were compared using one-way analysis of variance, followed by Tukey's *post-hoc* test. Different letters indicate significant differences ($P < 0.05$)

aogashimaense produced in potato dextrose broth (PDB) were applied to *Bgt* conidia in vitro (Fig. 5). In the control group, more than 90% of *Bgt* conidia germinated and 47% formed an appressorium. However, the proportion of germinated conidia in the *S. aogashimaense* exudate-treated group was 63%, which was significantly lower than that in the control group. Additionally, only 2% of *S. aogashimaense* exudate-treated conidia formed an appressorium.

S. aogashimaense decreases the biomass of *Bgt* on wheat leaves

To quantitatively evaluate the suppressive effects of *S. aogashimaense* on *Bgt*, the fungal mass on *Bgt*-infected wheat leaves inoculated with *S. aogashimaense* was measured via quantitative real-time polymerase chain reaction (qPCR) analysis (Fig. 6). Compared with that at 0 dpi, the biomasses of *S. aogashimaense* at 3, 6 and 9 dpi were increased by 26, 28 and 21 times, respectively (Fig. 6d). In contrast, the biomasses of *Bgt* at 3, 6 and 9 dpi were significantly decreased by 2.0, 5.7 and 3.9 times, respectively, when compared with that at 0 dpi (Fig. 6e).

Complete genome sequence of *S. aogashimaense*

The genome of *S. aogashimaense* was sequenced and annotated (Fig. 7). The size of the complete chromosome-scale genome of *S. aogashimaense* was 30.26 Mb (N_{50} value = 4.07 Mb) with 48.95% GC content and 98.6% completed benchmarking universal single-copy orthologs (BUSCOs) (Table 1). The number of protein-coding genes was 8963, which comprised 8688 annotated and 275 unannotated genes. The average gene length was 2350.55 bp. The genome comprised 94, 67 and 19 copies of tRNAs, rRNAs and snRNAs, respectively. Additionally, 2094 novel transcripts were annotated using RNA sequencing (RNA-seq) analysis (Additional file 1: Table S1).

Gene mining and Basic Local Alignment Search Tool analyses identified two putative effector-coding genes (*Sao008714* and *Sao006491*) (Additional file 2: Figures S1, S2). These two genes were significantly upregulated during the mycoparasitic interaction (Additional file 2: Figure S3). AntiSMASH (antibiotics & Secondary Metabolite Analysis Shell) analysis identified the gene clusters involved in the putative secondary metabolite biosynthesis in *S. aogashimaense*. Antibiotics and secondary metabolites produced by *S. aogashimaense* were also predicted (Additional file 1: Table S2). Among these, nine gene clusters exhibited marked hits (13–100% similarity) to different types of known secondary metabolite biosynthesis gene clusters, including those involved in the biosynthesis of terpene, non-ribosomal peptide synthetase and type I polyketide synthase.

Discussion

Mycoparasitism and antagonistic activity of *S. aogashimaense* against *Bgt*

The antagonistic effects of *Simplicillium* spp. on fungal phytopathogens have been previously reported (Ward et al. 2012; Gauthier et al. 2014; Shin et al. 2017; Teasdale et al. 2018; Wang et al. 2020; Wilson et al. 2020).

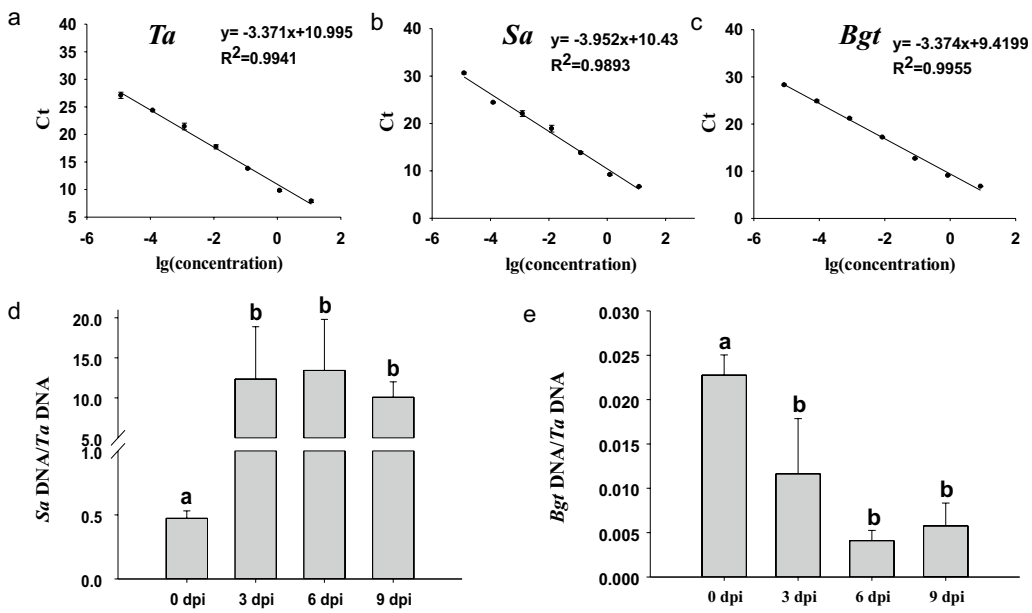

Fig. 6 Biomasses of *Simplicillium aogashimaense* and *Blumeria graminis* f. sp. *tritici* (*Bgt*) on wheat leaves at different time points. The DNA concentration standard curves of wheat (*Triticum aestivum*, *Ta*) (**a**), *S. aogashimaense* (*Sa*) (**b**) and *Bgt* (**c**) were used to calculate the biomasses of *S. aogashimaense* (**d**) and *Bgt* (**e**). The standard curves derived from serially diluted DNA samples were obtained using the primers of elongation factors of *Ta*, *Sa* and *Bgt*. Wheat leaves were inoculated with *Bgt* for 6 days, followed by inoculation with a suspension of *Sa* conidia for biomass calculation. Data are represented as mean ± standard deviation from three independent biological experiments. The means were compared using one-way analysis of variance, followed by Tukey's *post-hoc* test. Different letters indicate significant differences ($P < 0.05$)

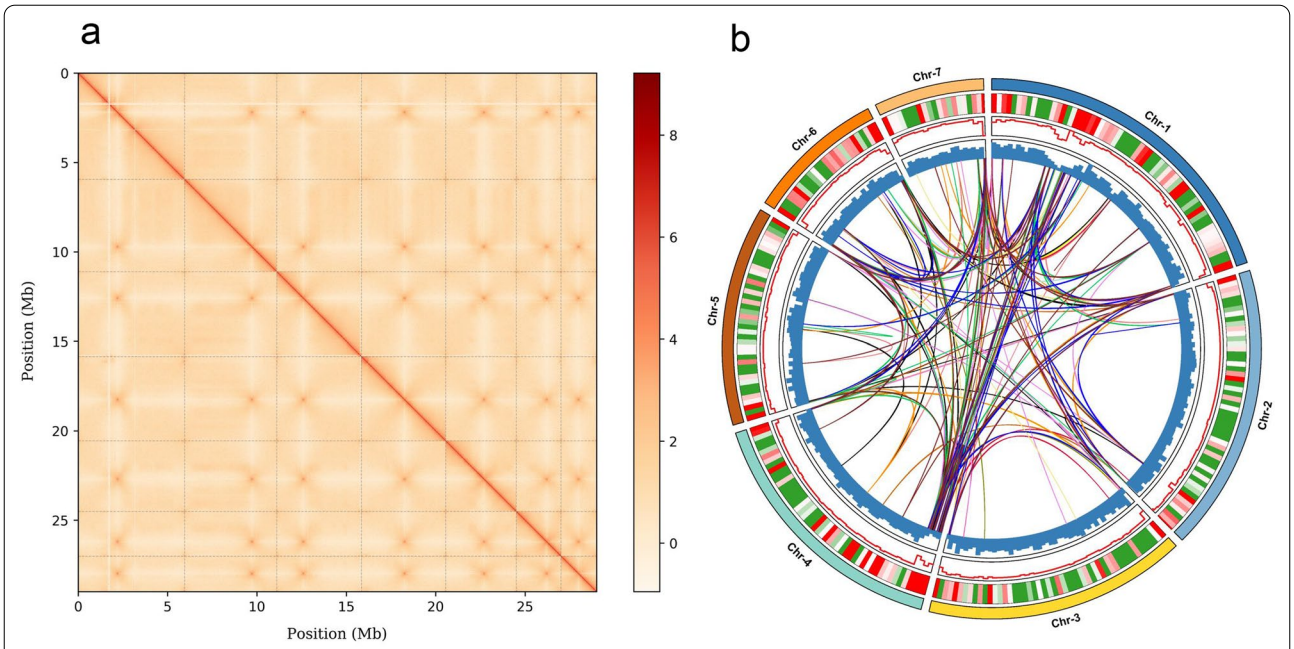

Fig. 7 *Simplicillium aogashimaense* genome assembly. **a** The Hi-C interaction heatmap for *S. aogashimaense*. The color in the figure from white to red indicates the increase in the intensity of interaction. **b** Overview of chromosomal features of the *S. aogashimaense* genome. The circular layers represent the following (from outside to inside): seven chromosomes (colored layers), repeat coverage (heatmap), GC content (red lines) and gene density (blue bars). Connected lines show the linked genes in *S. aogashimaense* chromosomes

Table 1 Characteristics of *S. aogashimaense* genome

Feature	Characteristics
Genome size (Mb)	30.26
N_{50} (Mb)	4.07
Complete BUSCOs (%)	99.3
Complete and single-copy BUSCOs (%)	98.6
GC content (%)	48.95
Protein coding genes	8963
Annotated genes	8688
Unannotated genes	275
Average gene length (bp)	2350.55
tRNA (copy)	94
rRNA (copy)	67
snRNA (copy)	19

However, most studies have focused on the antagonistic effects of *Simplicillium* spp. on rust or gray mold fungi. Limited studies have examined the suppressing effects of *Simplicillium* spp. on other phytopathogenic fungi. In particular, the antagonistic effects of *Simplicillium* spp. on the development of powdery mildew pathogens, including *Bgt* that causes economically and agriculturally important plant diseases, have not been evaluated. This study aimed to identify a BCA for *Bgt*. A mycoparasite of *Bgt* was identified and characterized under field conditions.

The mycoparasite distinctly interacted with *Bgt* (Fig. 1). Morphological and molecular analyses revealed that the mycoparasite was *S. aogashimaense* (Fig. 2). The color and morphology of the *Bgt* colonies changed upon infection with *S. aogashimaense*. Additionally, the *Bgt* colonies and conidiophores were disrupted upon *S. aogashimaense* infection. Thus, the direct antagonistic effect of *S. aogashimaense* on disrupting *Bgt* colonies and conidiophores was found. These results indicate that *S. aogashimaense* is a potential BCA for powdery mildew diseases. Previously, *S. aogashimaense* was found in soil samples or isolated from *Brachiaria brizantha* as a putative fungal endophyte (Nonaka et al. 2013; Teasdale et al. 2018). This study demonstrated that *S. aogashimaense* can parasitize *Bgt* colonies and efficiently suppressed the development of the wheat powdery mildew fungus. This indicated that *S. aogashimaenseis* is a natural BCA that exerts antagonistic effects on *Bgt*.

S. aogashimaense suppresses the growth of *Bgt*

To examine the suppressive effects of *S. aogashimaense* on *Bgt*, the development of this parasite on *Bgt* colonies was examined. *S. aogashimaense* directly wrapped around *Bgt* conidiophores and disrupted conidial distribution (Fig. 3). This further confirmed that *S. aogashimaense* can

suppress powdery mildew disease in wheat. To visualize the interactions between mycoparasites and *Bgt*, GFP was transformed into the BCAs to examine their effect on powdery mildew fungi (Lefebvre et al. 2013; Németh et al. 2019). Previously, *S. lanosoniveum* was transformed with GFP to monitor its infection processes in *Phakopsora pachyrhizi* (Gauthier et al. 2014). In this study, GFP transformation improved the visualization of mycoparasite structures of *S. aogashimaense*. *S. aogashimaense* formed dense mycelia and produced conidiophores on *Bgt* colonies and consequently inhibited the conidial distribution of *Bgt* (Fig. 4a–c). In some cases, the *Bgt* conidia exhibited a fluorescence signal, suggesting that *S. aogashimaense* can directly penetrate the structures of *Bgt* (Fig. 4g–i). Similar phenomenon was observed in other *Simplicillium* spp., which directly penetrate rust pathogens (Gauthier et al. 2014; Wang et al. 2020). In this study, GFP was stably expressed using the ATMT method (Fig. 4d–f). This indicates that the ATMT method can be applied for transforming physiologically and phylogenetically diverse *Simplicillium* spp. and for functional analyses of genes and proteins involved in mycoparasitism and metabolism.

In this study, the exudates of *S. aogashimaense* efficiently inhibited conidial gemination and appressorial differentiation (the pre-penetration processes) of *Bgt*. This suggests that *S. aogashimaense* produces growth-inhibitory components against *Bgt* (Fig. 5). These results are consistent with those of previous studies, which demonstrated that *S. lanosoniveum* releases growth-inhibitory substances against various phytopathogens. Previous studies have reported that *S. obclavatum* produces cyclic peptides with antifungal activities (Chen et al. 2017; Liang et al. 2017). The exudates of *S. aogashimaense* effectively suppressed the pre-penetration processes that are prerequisite for successful *Bgt* infection. Thus, the metabolites released from *S. aogashimaense* can be utilized as bio-fungicides for the management of powdery mildew diseases (Zabka et al. 2008; Hansjakob et al. 2010, 2012). Secondary metabolite biosynthesis gene cluster analysis revealed 41 gene clusters that were potentially related to antifungal, antibacterial and insecticidal compounds (Additional file 1: Table S2). Three gene clusters were similar to those involved in the biosynthesis of trichodiene (13% similarity), squalestatin 1 (40% similarity) and AbT 1 (100% similarity), which are reported to exhibit antifungal activities (Baxter et al. 1992; Jones et al. 1992; Hasumi et al. 1993; Bills et al. 1994; Blows et al. 1994; Slightom et al. 2009; Tijerino et al. 2011; Malmierca et al. 2015a, b). However, the specific antifungal agents in exudates of *S. lanosoniveum* are not known. Further studies are needed to screen the efficient metabolites of *S. aogashimaense* for fungal phytopathogen control.

Consistent with the microscopic observations, the biomass of *S. aogashimaense* significantly increased from 3 dpi, while that of *Bgt* markedly decreased from 3 dpi (Fig. 6). Previous studies also demonstrated the direct colonization and disease suppressive effects of *Simplicillium* spp. on rust pathogens (Gauthier et al. 2014; Wang et al. 2020). The findings of this study indicate that *S. aogashimaense*, a natural mycoparasite, can be an effective BCA for powdery mildew. However, the environmental factors affecting the mycoparasitism of *S. aogashimaense* on phytopathogens have not been completely elucidated. Further studies are needed to determine the optimal conditions for *S. aogashimaense* development to enable the application of this parasitic fungus for phytopathogen management under field conditions.

Genome of *S. aogashimaense*

At least 15 *Simplicillium* species have been currently identified. Some members of this genus exhibit growth-inhibitory activities against phytopathogens (Chen et al. 2019). However, the information on the genome of *Simplicillium* species is limited. Jauregui et al. (2020) reported a draft genome of *S. aogashimaense*, the only available genome for *Simplicillium* species, however, the parasitic mechanism and/or the discovery of antifungal secondary metabolites in *S. aogashimaense* cannot be deeply mined owing to the limited assembly and annotation of the draft genome. Therefore, the genome of *S. aogashimaense* was sequenced, assembled and annotated at the chromosomal level in this study (Fig. 7). The genome size of the test strain was 30.26 Mb, which is slightly larger than the previously reported draft genome of *S. aogashimaense* (strain 72–15.1) (Jauregui et al. 2020). Additionally, the genome comprised 8963 protein-coding genes. RNA-seq analysis revealed 2094 novel transcripts. This indicates that the gene expression patterns in *S. aogashimaense* vary. Genome data provided novel insights into the genomic features of *S. aogashimaense*, which can be applied for mining key genes related to mycoparasitic processes and antifungal secondary metabolites. Previously, the effectors involved in the interaction between *Pseudozyma flocculosa* and *B. graminis* have been elucidated using genome and RNA sequencing (Laur et al. 2018). *Sao008714* and *Sao006491* were putative effector-coding genes, which were highly similar to their homologs in *P. flocculosa* and *Trichoderma* spp. (Additional file 2: Figures S1, S2). The expression levels of *Sao008714* and *Sao006491* were significantly upregulated from 3 dpi (Additional file 2: Figure S3). *Trichoderma* spp. are reported to act as BCAs for various phytopathogens (Harman 2006; Moya et al. 2020; Sood et al. 2020; Zin and Badaluddin 2020). Therefore, these two genes, which putatively

code for effectors, may play crucial roles in mycoparasitic interactions. Effectors are reported to play crucial roles in phytopathogen-host and mycoparasitic agent-phytopathogen systems (Laur et al. 2018; Li et al. 2021; Yuan et al. 2021). However, the effectors and their mechanisms in the interaction between *S. aogashimaense* and *Bgt* have not been elucidated. The effectors in *S. aogashimaense* and their functions during mycoparasitism should be elucidated in the future.

Conclusions

This study provides novel insights into the host range and developmental niches of *S. aogashimaense* that parasitizes *Bgt* colonies and helps fill knowledge gaps in the understanding of the interaction between *S. aogashimaense* and *B. graminis*. The major findings of this study are as follows: (1) *S. aogashimaense* directly inhibits conidiophore formation and conidial distribution of *Bgt*; (2) *S. aogashimaense* decreases the biomass of *Bgt* during parasitic interaction, demonstrating its potential application in the management of wheat powdery mildew; (3) the visualization of *S. aogashimaense* is improved with GFP transformation using the ATMT method, which can be applied for genetic modification of *Simplicillium* spp.; (4) the exudates of *S. aogashimaense* suppressed conidial germination and appressorial differentiation (the pre-penetration processes) of *Bgt*; (5) the chromosome-scale genome assembly of *S. aogashimaense* revealed distinct features that can be used for mining key genes in future studies.

Methods

Fungal and plant materials

Wheat (cv. Aikang 58) was sown in plastic pots (9 cm in diameter) filled with soil collected from the field and maintained in growth chambers at 18 °C, with a light intensity of 200 μmol photons/m^2s and a photoperiod of 16-h light/8-h dark and 70% relative humidity. *Bgt* was propagated on its host plants under the same conditions. One day before inoculation, heavily infected host leaves were warily shaken to remove older *Bgt* conidia, and freshly formed spores were then used for further experimentation.

The mycoparasite was isolated from *Bgt*-infected wheat leaves at a cultivation field and cultured on PDA medium at 25 °C in the dark until fungal colonies appeared. To obtain a pure strain, individual spores of the mycoparasite were isolated and transferred onto PDA medium to allow colony development at 25 °C in the dark. Isolation was conducted twice and the purified strain was used for further assays.

Microscopic observation

To determine morphological characteristics, the mycoparasite was initially imaged under a light microscope (Sunny Optical, EX30, Zhejiang, China) and the images were analyzed using ImageJ software. The fungal structures were examined under a scanning electron microscope (Hitachi TM3030Plus, Japan) following a previously reported method (Zhu et al. 2020a).

DNA extraction and amplification

Total genomic DNA was isolated from the mycoparasite according to a previously reported method (Zhu et al. 2019). The ITS region of rDNA was PCR amplified with ITS1/ITS4 primer pairs (White et al. 1990). PCR was performed using a C1000 TouchTM Thermal Cycler (Bio-Rad, Hercules, California, United States). The PCR conditions were as follows: 94 °C for 5 min, followed by 35 cycles of 94 °C for 30 s, 55 °C for 30 s, 72 °C for 1 min and a final elongation at 72 °C for 5 min. The amplicon was sequenced (Invitrogen, Shanghai, China) and the sequence was deposited in GenBank (Accession no. MT936440).

Phylogenetic analysis

The ITS sequences of *Simplicillium* spp. were retrieved from the National Center for Biotechnology Information (NCBI, https://www.ncbi.nlm.nih.gov/) database and aligned using ClustalW in MEGA software (version 10.1.8). The phylogenetic tree was constructed using MEGA software. The maximum likelihood method was used for phylogenetic tree construction with the options of 1000 bootstrap replicates, Tamura-Nei model and 50% site coverage cut off. The ITS sequences of *Arthrocladiella mougeotii* and *Erysiphe* sp. were used as the outgroup (Zhu et al. 2020b, c).

Hyperparasitism assays

The leaves of 14-day-old wheat seedlings (cv. Aikang 58) were inoculated with *Bgt* conidia and incubated in a growth chamber under the conditions described above. At 6 dpi, plants were inoculated with spore suspension (1×10^6 spores/mL) of the identified *S. aogashimaense* and the inoculated plants were incubated in a growth chamber. *Bgt*-inoculated plants treated with water served as controls. At 3, 6 and 9 dpi, the leaves were collected for microscopic analysis. The leaves were bleached to observe *Bgt* and *S. aogashimaense* under a light microscope (Zhu et al. 2017). The fungal structures were stained with trypan blue in acetic acid/water/glycerol (1:1:1, v/v/v) for 1 h.

Fungal biomass determination

To determine the effect of *S. aogashimaense* on *Bgt* biomass, *Bgt*-infected leaves were treated with water or *S. aogashimaense* spore suspension (1×10^6 spores/mL). At 3, 6 and 9 dpi, DNA was isolated from the samples using TRIzol reagent, following the manufacturer's instructions (Invitrogen). The DNA was stored at -80 °C until qPCR analysis. The elongation factor 1(EF1) alpha-encoding genes of wheat, *S. aogashimaense* and *Bgt* were amplified with the following primers: wheat EF1, TGGTGT CATCAAGCCTGGTATGGT (forward) and ACTCAT GGTGCATCTCAACGGACT (reverse); *S. aogashimaense* EF1, ATGGGTTGCGCTTCCTTCAA (forward) and GACGATGGCAGAGTCACCGTT (reverse); *Bgt* EF1, AAGCTAAAGGCCGAACGTGA (forward) and GCACAGTCAGCTTGAGAGGT (reverse) (Coram et al. 2008; Hu et al. 2018). To generate the standard curves, the fusion plasmids of wheat EF1, *Bgt* EF1 and *S. aogashimaense* EF1 were serially diluted and subjected to qPCR analysis with selective primers to obtain the cycle threshold (Ct) values. The biomasses of wheat, *Bgt* and *S. aogashimaense* were calculated according to the corresponding standard curves. All qPCR experiments were conducted using a LightCycler 96 real-time PCR instrument (Roche, Switzerland). The PCR conditions were as follows: 95 °C for 15 min, followed by 45 cycles of 95 °C for 10 s and 60 °C for 30 s.

Pre-penetration processes of *Bgt*

To determine the effect of *S. aogashimaense* exudates on *Bgt* conidial germination and appressorial differentiation in vitro, *S. aogashimaense* was inoculated onto PDA and harvested at 20 dpi. PDA with *S. aogashimaense* (Ø = 1 cm) was then placed in a centrifuge tube with PDB and incubated on a shaker (150 rpm) at 20 °C for 6 days. Next, total PDB with white fungal structures was filtered through a filter paper (Ø = 7 cm, Newstar, Hangzhou, China) and a 0.22 μm syringe filter (Jinteng, Tianjin, China). The resulting solution containing *S. aogashimaense* exudates was stored at 4 °C for further experiments. To observe the prepenetration processes of *Bgt*, Formvar®/wheat wax-coated glass slides were prepared according to a previously described method (Zhu et al. 2017). Briefly, wheat leaf wax was isolated using chloroform and mixed with Formvar® (w/v = 0.5%). Cleaned glass slides were dipped into the Formvar®/wheat wax solution for 15 s and dried at room temperature for 24 h. The *S. aogashimaense* exudate (treated group) or filtered PDB (control group) was sprayed onto Formvar® wheat wax-coated slides and dried for at least 12 h. *Bgt* conidia were inoculated onto glass slides and incubated for 18 h according to a previously reported method (Zhu et al. 2019). Individual conidia on the surface of each slide were observed under a light microscope to determine whether the spores remained non-germinated, had formed a primary germ tube, a secondary germ tube, a swollen appressorial germ tube or an appressorium. Only individual, well-separated conidia were counted in each experiment to eliminate the possible inhibition caused by crowding.

Chromosome-scale genome assembly of *S. aogashimaense*

To sequence the *S. aogashimaense* genome, genomic DNA was extracted from the colonies at 25 dpi using the cetyltrimethylammonium bromide method. Single-molecule real-time libraries were constructed and sequenced using a PacBio Sequel II instrument (Pacific Biosciences, Menlo Park, CA, USA) at Frasergen Bioinformatics Co., Ltd. (Wuhan, China). In total, 31.33 G polymerase reads for raw data and 31.1 G subreads for clean data were obtained after the removal of adaptor sequences from the sequencing data. RNA-seq was performed to sequence the full-length transcripts using Illumina® sequencing. *S. aogashimaense* RNA was extracted from the same colonies using TRIzol reagent (Invitrogen) following the manufacturer's instructions. RNA-seq libraries were prepared using the NEBNext® Ultra™ RNA Library Prep Kit for Illumina® (NEB, USA) following the manufacturer's instructions. The libraries were sequenced on the Novaseq 6000 platform at Frasergen Bioinformatics Co., Ltd. (Wuhan, China).

Pseudochromosomes (superscaffolds) were determined using Hi-C analysis as described previously (Dudchenko et al. 2017). Briefly, 11 Gb of clean read pairs were obtained from the Hi-C library and mapped to the polished *S. aogashimaense* contig assembly using Juicer (version: 1.6) with default parameters (Durand et al. 2016). The LACHESIS tool (Burton et al. 2013) was used to cluster contigs (n = 18) into chromosome-level scaffolds using the genomic proximity signal of Hi-C data.

GFP transformation

To transform *S. aogashimaense*, the binary vector pPK-2Tgfp (Martínez-Cruz et al. 2016) was transferred into the *A. tumefaciens* strain GV3101.The transferred strain was cultured in 2 mL of YEP medium containing 50 μg/mL kanamycin and 50 μg/mL gentamicin in an orbital shaker at 140 rpm and 28 °C for 24 h. Next, the *A. tumefaciens* strain was directly pipetted onto *S. aogashimaense* culture grown on PDA and incubated for 4 days at room temperature (Németh et al. 2019). Subsequently, the spores of *S. aogashimaense* were inoculated onto PDA medium containing 50 μg/mL carbendazim and 100 μg/mL cefotaxime and incubated for 10 days at room temperature. Newly formed colonies, which were

transformed *S. aogashimaense* colonies, were observed under a fluorescence microscope (BX63, Olympus, Japan).

Abbreviations

Agt: Swollen appressorial germ tube; App: Appressorium; ATMT: *Agrobacterium tumefaciens*-mediated transformation; BCAs: Biocontrol agents; *Bgt*: *Blumeria graminis* f. sp. *tritici*; Ct: Cycle threshold; dpi: Days post-inoculation; GFP: Green fluorescent protein; ITS: Internal transcribed spacer; Ng: Non-germinated conidium; PDA: Potato dextrose agar; PDB: Potato dextrose broth; Pgt: Primary germ tube; *Sa*: *S. aogashimaense*; Sgt: Secondary germ tube; *Ta*: *Triticum aestivum*.

Supplementary Information

The online version contains supplementary material available at https://doi.org/10.1186/s42483-022-00121-5.

Additional file 1: Table S1. Novel transcript annotation of *Simplicillium aogashimaense*. **Table S2.** AntiSMASH analysis of secondary metabolite biosynthesis gene clusters in *Simplicillium aogashimaense*. The genome-wide identification, annotation and analysis of secondary metabolite biosynthesis gene clusters in *S. aogashimaense* were performed following a previously described method (Blin et al. 2019).

Additional file 2: Figure S1. Alignment (**a**) and phylogenetic analysis (**b**) of Sao008714 and its homologs from *Trichoderma* spp. and *Pseudozyma flocculosa* were performed using DNAMAN and MEGA, respectively. The evolutionary tree was constructed using the maximum likelihood method with the options of 1000 bootstrap replicates, Tamura-Nei model and 50% site coverage cut off (Zhu et al. 2022). **Figure S2**. Alignment (**a**) and phylogenetic analysis (**b**) of Sao006491 and its homologs from *Trichoderma* spp. and *Pseudozyma flocculosa* were performed using DNAMAN and MEGA, respectively. The evolutionary tree was constructed according to Maximum likelihood method with the options of 1000 bootstrap replicates, Tamura-Nei model and 50% site coverage cut-off. **Figure S3**. The expression levels of *Sao008714* (**a**) and *Sao006491* (**b**) during mycoparasitic interaction of *S. aogashimaense* with *Blumeria graminis* f. sp. *tritici* (*Bgt*). The spore suspension of *S. aogashimaense* was sprayed onto wheat leaves with *Bgt* colonies. The whole leaves were harvested at 3, 6 and 9 dpi for RNA extraction. The elongation factor 1 alpha-encoding gene of *S. aogashimaense* was used as the reference gene. The following primers were used for amplification: Sao006491, GGATATGAGTCGCGCTTCCA (forward) and AAACTGAGCGGCGTTTGTTCF (reverse); Sao008714, ACAATCCAT CGGCCACAGAG (forward) and CCAACTCCGCCATGAGATGT (reverse). The expression levels of *Sao008714* and *Sao006491* were calculated using the $2^{-\Delta\Delta Ct}$ method. Data are expressed as mean ± standard deviation from three independent biological experiments. The means were compared using one-way analysis of variance, followed by Tukey's *post hoc* test. Different letters indicate significant differences ($P < 0.05$).

Acknowledgements

We would like to thank Prof. Alejandro Pérez-García from University of Malaga for sharing the vector pPK2Tgfp and Prof. Zhengang Ru from Henan Institute of Science and Technology for sharing the wheat (cv. Aikang 58) seeds.

Authors' contributions

MZ: Conceptualization, methodology, writing, reviewing and editing, funding acquisition and supervision. XD: Investigation, validation, software, visualization and writing original draft preparation. PKC: Investigation and software. YFL: Methodology. ZBQ: Conceptualization and methodology. All authors read and approved the final manuscript.

Funding

This work was financially supported by Foundation for the Key Research Program of Higher Education of Henan (20A210026), Doctor Initiative Foundation of Henan Normal University to Mo Zhu (5101049170196), Open Project of Key Laboratory of Integrated Pest Management on Crops in Central China, Ministry of Agriculture and Rural Affairs, P. R. China and Hubei Key Laboratory of Crop Disease, Insect Pests and Weeds Control (2020ZTSJJ3) and Open Project of research on typical aquatic plant remediation techniques for rural water pollution (FIRI20210301).

Availability of data and materials

Raw sequencing reads of *Simplicillium aogashimaense* genome reported in this study were deposited into the public database of NCBI (BioProject accession no. PRJNA793154). RNA-seq raw data was also deposited under PRJNA793154.

Declarations

Ethics approval and consent to participate

Not applicable.

Consent for publication

Not applicable.

Competing interests

The authors declare that they have no competing interests.

Author details

[1]College of Life Sciences, Henan Normal University, 46# East of Construction Road, Xinxiang 453007, Henan, People's Republic of China. [2]Henan International Joint Laboratory of Agricultural Microbial Ecology and Technology, Henan Normal University, Xinxiang 453007, People's Republic of China.

Received: 4 January 2022 Accepted: 19 April 2022
Published online: 06 May 2022

References

Baxter A, Fitzgerald BJ, Hutson JL, McCarthy AD, Motteram JM, Ross BC, et al. Squalestatin 1, a potent inhibitor of squalene synthase, which lowers serum cholesterol *in vivo*. J Biol Chem. 1992;267:11705–8. https://doi.org/10.1016/S0021-9258(19)49754-8.

Belanger RR, Labbe C, Lefebvre F, Teichmann B. Mode of action of biocontrol agents: all that glitters is not gold. Can J Plant Pathol. 2012;34:469–78. https://doi.org/10.1080/07060661.2012.726649.

Bills GF, Peláez F, Polishook JD, Diez-Matas MT, Harris GH, Clapp WH, et al. Distribution of zaragozic acids (squalestatins) among filamentous ascomycetes. Mycol Res. 1994;98:733–9. https://doi.org/10.1016/S0953-7562(09)81046-0.

Blin K, Shaw S, Steinke K, Villebro R, Ziemert N, Lee SY, et al. antiSMASH 5.0: updates to the secondary metabolite genome mining pipeline. Nucleic Acids Res. 2019;47:W81–7. https://doi.org/10.1093/nar/gkz310.

Blows WM, Foster G, Lane SJ, Noble D, Piercey JE, Sidebottom PJ, et al. The squalestatins, novel inhibitors of squalene synthase produced by a species of *Phoma*. V. Minor metabolites. J Antibiot (tokyo). 1994;47:740–54. https://doi.org/10.7164/antibiotics.47.740.

Burton JN, Adey A, Patwardhan RP, Qiu R, Kitzman JO, Shendure J. Chromosome-scale scaffolding of de novo genome assemblies based on chromatin interactions. Nat Biotechnol. 2013;31:1119–25. https://doi.org/10.1038/nbt.2727.

Chen RS, Huang CC, Li JC, Tsay JG. Evaluation of characteristics of *Simplicillium lanosoniveumon* pathogenicity to aphids and *in vitro* antifungal potency against plant pathogenic fungi. Int J Environ Res. 2017;3:55–61.

Chen WH, Liu C, Han YF, Liang JD, Tian WY, Liang ZQ. Three novel insect-associated species of *Simplicillium* (Cordycipitaceae, Hypocreales) from Southwest China. MycoKeys. 2019;58:83–102. https://doi.org/10.3897/mycokeys.58.37176.

Coram TE, Wang M, Chen X. Transcriptome analysis of the wheat-*Puccinia striiformis* f. sp. *tritici* interaction. Mol Plant Pathol. 2008;9:157–69. https://doi.org/10.1111/j.1364-3703.2007.00453.x.

Dean R, Van Kan JAL, Pretorius ZA, Hammond-Kosack KE, Di Pietro A, Spanu PD, et al. The top 10 fungal pathogens in molecular plant pathology. Mol

Plant Pathol. 2012;13:414–30. https://doi.org/10.1111/j.1364-3703.2011.00783.x.
Dik AJ, Verhaar MA, Bélanger RR. Comparison of three biological control agents against cucumber powdery mildew (*Sphaerotheca fuliginea*) in semi-commercial-scale glasshouse trials. Eur J Plant Pathol. 1998;104:413–23. https://doi.org/10.1023/A:1008025416672.
Dudchenko O, Batra SS, Omer AD, Nyquist SK, Hoeger M, Durand NC, et al. De novo assembly of the *Aedes aegypt* genome using Hi-C yields chromosome-length scaffolds. Science. 2017;356:92–5. https://doi.org/10.1126/science.aal3327.
Durand NC, Shamim MS, Machol I, Rao SSP, Huntley MH, Lander ES, et al. Juicer provides a one-click system for analyzing loop-resolution Hi-C experiments. Cell Syst. 2016;3:95–8. https://doi.org/10.1016/j.cels.2016.07.002.
Gauthier NW, Maruthachalam K, Subbarao KV, Brown M, Xiao Y, Robertson CL, et al. Mycoparasitism of *Phakopsora pachyrhizi*, the soybean rust pathogen, by *Simplicillium lanosoniveum*. Biol Control. 2014;76:87–94. https://doi.org/10.1016/j.biocontrol.2014.05.008.
Hansjakob A, Bischof S, Bringmann G, Riederer M, Hildebrandt U. Very-long-chain aldehydes promote *in vitro* prepenetration processes of *Blumeria graminis* in a dose-and chain length-dependent manner. New Phytol. 2010;188:1039–54. https://doi.org/10.1111/j.1469-8137.2010.03419.x.
Hansjakob A, Riederer M, Hildebrandt U. Appressorium morphogenesis and cell cycle progression are linked in the grass powdery mildew fungus *Blumeria graminis*. Fungal Biol. 2012;116:890–901. https://doi.org/10.1016/j.funbio.2012.05.006.
Harman GE. Overview of mechanisms and uses of *Trichoderma* spp. Phytopathology®. 2006;96:190–4. https://doi.org/10.1094/phyto-96-0190.
Hasumi K, Tachikawa K, Sakai K, Murakawa S, Yoshikawa N, Kumazawa S, et al. Competitive inhibition of squalene synthetase by squalestatin 1. J Antibiot (tokyo). 1993;46:689–91. https://doi.org/10.7164/antibiotics.46.689.
Hu Y, Liang Y, Zhang M, Tan F, Zhong S, Li X, et al. Comparative transcriptome profiling of *Blumeria graminis* f. sp. *tritici* during compatible and incompatible interactions with sister wheat lines carrying and lacking Pm40. PLoS ONE. 2018;13:e0198891. https://doi.org/10.1371/journal.pone.0198891.
Jankovics T, Komáromi J, Fábián A, Jäger K, Vida G, Kiss L. New insights into the life cycle of the wheat powdery mildew: direct observation of ascosporic infection in *Blumeria graminis* f. sp. *tritici*. Phytopathology®. 2015;105:797–804. https://doi.org/10.1094/phyto-10-14-0268-r.
Jauregui R, Johnson LJ, Teasdale SE. Draft genome sequence of *Simplicillium aogashimaense* 72–15.1, a putative endophyte of *Brachiaria brizantha*. Microbiol Resour Announce. 2020;9:e00366-20. https://doi.org/10.1128/mra.00366-20.
Jones CA, Sidebottom PJ, Cannell RJ, Noble D, Rudd BA. The squalestatins, novel inhibitors of squalene synthase produced by a species of *Phoma*. III. Biosynthesis. J Antibiot (tokyo). 1992;45:1492–8. https://doi.org/10.7164/antibiotics.45.1492.
Kiss L. A review of fungal antagonists of powdery mildews and their potential as biocontrol agents. Pest Manag Sci. 2003;59:475–83. https://doi.org/10.1002/ps.689.
Köhl J, de Geijn HG, Haas LG, Henken B, Hauschild R, Hilscher U, et al. Stepwise screening of candidate antagonists for biological control of *Blumeria graminis* f. sp. *tritici*. Biol Control. 2019;136:104008. https://doi.org/10.1016/j.biocontrol.2019.104008.
Laur J, Ramakrishnan GB, Labbé C, Lefebvre F, Spanu PD, Bélanger RR. Effectors involved in fungal-fungal interaction lead to a rare phenomenon of hyperbiotrophy in the tritrophic system biocontrol agent-powdery mildew-plant. New Phytol. 2018;217:713–25. https://doi.org/10.1111/nph.14851.
Lefebvre F, Joly DL, Labbé C, Teichmann B, Linning R, Belzile F, et al. The transition from a phytopathogenic smut ancestor to an anamorphic biocontrol agent deciphered by comparative whole-genome analysis. Plant Cell. 2013;25:1946–59. https://doi.org/10.1105/tpc.113.113969.
Li X, Jin C, Yuan H, Huang W, Liu F, Fan R, et al. The barley powdery mildew effectors CSEP0139 and CSEP0182 suppress cell death and promote *B graminis* fungal virulence in plants. Phytopathol Res. 2021;3:7. https://doi.org/10.1186/s42483-021-00084-z.
Liang X, Nong XH, Huang ZH, Qi SH. Antifungal and antiviral cyclic peptides from the deep-sea-derived fungus *Simplicillium obclavatum* EIODSF 020. J Agric Food Chem. 2017;65:5114–21. https://doi.org/10.1021/acs.jafc.7b01238.
Malmierca MG, McCormick SP, Cardoza RE, Alexander NJ, Monte E, Gutiérrez S. Production of trichodiene by *Trichoderma harzianum* alters the perception of this biocontrol strain by plants and antagonized fungi. Environ Microbiol. 2015;17:2628–46. https://doi.org/10.1111/1462-2920.12506.
Malmierca MG, McCormick SP, Cardoza RE, Monte E, Alexander NJ, Gutiérrez S. Trichodiene production in a *Trichoderma harzianum erg1*-silenced strain provides evidence of the importance of the sterol biosynthetic pathway in inducing plant defense-related gene expression. Mol Plant Microbe in®. 2015;28:1181–97. https://doi.org/10.1094/mpmi-06-15-0127-r.
Martínez-Cruz J, Romero D, Vicente A, Pérez-García A. Transformation of the cucurbit powdery mildew pathogen *Podosphaera xanthii* by *Agrobacterium tumefaciens*. New Phytol. 2016. https://doi.org/10.1111/nph.14297.
Matzen N, Heick TM, Jørgensen LN. Control of powdery mildew (*Blumeria graminis* spp.) in cereals by Serenade®ASO (*Bacillus amyloliquefaciens* (former *subtilis*) strain QST 713). Biol Control. 2019;139:104067. https://doi.org/10.1016/j.biocontrol.2019.104067.
Moya P, Barrera V, Cipollone J, Bedoya C, Kohan L, Toledo A, et al. New isolates of *Trichoderma* spp. as biocontrol and plant growth-promoting agents in the pathosystem *Pyrenophora teres*-barley in Argentina. Biol Control. 2020;141:104152. https://doi.org/10.1016/j.biocontrol.2019.104152.
Németh MZ, Pintye A, Horváth ÁN, Vági P, Kovács GM, Gorfer M, et al. Green fluorescent protein transformation sheds more light on a widespread mycoparasitic interaction. Phytopathology®. 2019;109:1404–16. https://doi.org/10.1094/phyto-01-19-0013-r.
Neveu B, Labbé C, Bélanger RR. GFP technology for the study of biocontrol agents in tritrophic interactions: a case study with *Pseudozyma flocculosa*. J Microbiol Methods. 2007;68:275–81. https://doi.org/10.1016/j.mimet.2006.08.012.
Nonaka K, Kaifuchi S, Ōmura S, Masuma R. Five new *Simplicillium* species (Cordycipitaceae) from soils in Tokyo. Japan Mycoscience. 2013;54:42–53. https://doi.org/10.1016/j.myc.2012.07.002.
Shin TS, Yu NH, Lee J, Choi GJ, Kim JC, Shin CS. Development of a biofungicide using a mycoparasitic fungus *Simplicillium lamellicola* BCP and its control efficacy against gray mold diseases of tomato and ginseng. Plant Pathology J. 2017;33:337–44. https://doi.org/10.5423/PPJ.FT.04.2017.0087.
Siozios S, Tosi L, Ferrarini A, Ferrari A, Tononi P, Bellin D, et al. Transcriptional reprogramming of the mycoparasitic fungus *Ampelomyces quisqualis* during the powdery mildew host-induced germination. Phytopathology®. 2015;105:199–209. https://doi.org/10.1094/phyto-01-14-0013-r.
Slightom JL, Metzger BP, Luu HT, Elhammer AP. Cloning and molecular characterization of the gene encoding the Aureobasidin a biosynthesis complex in *Aureobasidium pullulans* BP-1938. Gene. 2009;431:67–79. https://doi.org/10.1016/j.gene.2008.11.011.
Sood M, Kapoor D, Kumar V, Sheteiwy MS, Ramakrishnan M, Landi M, et al. *Trichoderma*: the "secrets" of a multitalented biocontrol agent. Plants. 2020;9:762. https://doi.org/10.3390/plants9060762.
Teasdale SE, Caradus JR, Johnson LJ. Fungal endophyte diversity from tropical forage grass *Brachiaria*. Plant Ecol Divers. 2018;11:611–24. https://doi.org/10.1080/17550874.2019.1610913.
Tijerino A, Elena Cardoza R, Moraga J, Malmierca MG, Vicente F, Aleu J, et al. Overexpression of the trichodiene synthase gene *tri5* increases trichodermin production and antimicrobial activity in *Trichoderma brevicompactum*. Fungal Genet Biol. 2011;48:285–96. https://doi.org/10.1016/j.fgb.2010.11.012.
Wang N, Fan X, Zhang S, Liu B, He M, Chen X, et al. Identification of a hyperparasitic *Simplicillium obclavatum* strain affecting the infection dynamics of *Puccinia striiformis* f. sp. *tritici* on wheat. Front Microbiol. 2020;11:1277. https://doi.org/10.3389/fmicb.2020.01277.
Ward NA, Robertson CL, Chanda AK, Schneider RW. Effects of *Simplicillium lanosoniveum* on *Phakopsora pachyrhizi*, the soybean rust pathogen, and its use as a biological control agent. Phytopathology®. 2012;102:749–60. https://doi.org/10.1094/phyto-01-11-0031.
Wei DP, Wanasinghe DN, Hyde KD, Mortimer PE, Xu J, Xiao YP, et al. The genus *Simplicillium*. Mycokeys. 2019;60:69–92. https://doi.org/10.3897/mycokeys.60.38040.
White TJ, Bruns T, Lee S, Taylor J. PCR protocols: a guide to methods and applications. San Diego: Academic Press; 1990. p. 315.
Wilson A, Cuddy WS, Park RF, Harm GFS, Priest MJ, Bailey J, et al. Investigating hyperparasites as potential biological control agents of rust pathogens on cereal crops. Australas Plant Pathol. 2020;49:231–8. https://doi.org/10.1007/s13313-020-00695-8.

Yuan H, Jin C, Pei H, Zhao L, Li X, Li J, et al. The powdery mildew effector CSEP0027 interacts with barley catalase to regulate host immunity. Front Plant Sci. 2021. https://doi.org/10.3389/fpls.2021.733237.
Zabka V, Stangl M, Bringmann G, Vogg G, Riederer M, Hildebrandt U. Host surface properties affect prepenetration processes in the barley powdery mildew fungus. New Phytol. 2008;177:251–63. https://doi.org/10.1111/j.1469-8137.2007.02233.x.
Zhu M, Riederer M, Hildebrandt U. Very-long-chain aldehydes induce appressorium formation in ascospores of the wheat powdery mildew fungus *Blumeria graminis*. Fungal Biol. 2017;121:716–28. https://doi.org/10.1016/j.funbio.2017.05.003.
Zhu M, Riederer M, Hildebrandt U. UV-C irradiation compromises conidial germination, formation of appressoria, and induces transcription of three putative photolyase genes in the barley powdery mildew fungus, *Blumeria graminis* f. sp. *hordei*. Fungal Biol. 2019;123:218–30. https://doi.org/10.1016/j.funbio.2018.12.002.
Zhu M, Ji J, Wang M, Zhao M, Yin Y, Kong J, et al. Cuticular wax of mandarin fruit promotes conidial germination and germ tube elongation, and impairs colony expansion of the green mold pathogen, *Penicillium digitatum*. Postharvest Biol Technol. 2020a;169:111296. https://doi.org/10.1016/j.postharvbio.2020.111296.
Zhu M, Ji J, Zhao M, Chai J, Li YF. First report of powdery mildew caused by an *Erysiphe* sp. on *Aristolochia debilis* in China. Plant Dis. 2020b;104:2028. https://doi.org/10.1094/pdis-01-20-0007-pdn.
Zhu M, Zhao M, Ji J, Yang C, Chai J, Li Y. First report of *Arthrocladiella mougeotii* causing powdery mildew on *Lycium chinense* Mill. in Henan, China. Plant Dis. 2020c;104:3071. https://doi.org/10.1094/pdis-02-20-0445-pdn.
Zhu M, Duan X, Zeng Q, Cai P, Shi W, Qiu Z. *Podosphaera xanthii* causing powdery mildew on *Impatiens balsamina* in China. Can J Plant Pathol. 2022. https://doi.org/10.1080/07060661.2021.2011421.
Zin NA, Badaluddin NA. Biological functions of *Trichoderma* spp. for agriculture applications. Ann Agric Sci. 2020;65:168–78. https://doi.org/10.1016/j.aoas.2020.09.003.

Publisher's Note